

A Theoretical Study on Diffusion in Pulsating Flow

ESTRELLA B. FAGELA-ALABASTRO and J. D. HELLUMS

Rice University, Houston, Texas

A theoretical study has been made on the effect of pulsations in the flow field on interphase mass transfer. The phenomenon is of interest in studies of the cardiovascular system as well as in traditional engineering applications. The physical situation studied corresponds to fully developed flow in a long conduit with a periodic pressure gradient. The mass transfer problem was solved analytically for low amplitude pulsations for the two limiting cases of very small and very large frequencies. In addition, several numerical solutions were developed in the intermediate region where the asymptotic solutions are least accurate. The solutions taken together give a good quantitative overall view of the phenomenon.

One of the most interesting and unexpected results is that at very low frequencies it is possible for a pulsatile flow to yield a lower interphase mass flux than a steady Poiseuille flow with the same velocity.

Interphase mass transfer in pulsating flows is of interest in many areas of application including chemical reactor design, studies on flow transients using probes based on diffusion controlled electrode reactions, and studies on transport in the cardiovascular system. There has been surprisingly little work on this interesting class of problems or on the closely related heat transfer problem. A few of the more important studies including flow in conduits will be briefly described. Experiments were conducted by West and Taylor (7) on pulsating laminar flow in pipes and the results of their studies showed no appreciable increase in the heat flux. In turbulent flow, a 70% increase in the heat transfer coefficient was obtained at a pulse frequency of 100 cycles/min. Havemann and Narayan Rao (2) did experimental investigations on pulsating turbulent flows in pipes. They observed an increase in the heat flux over the steady state value when the frequency is greater than a critical frequency and a decrease in flux for lower frequencies. Mueller (5) also performed experiments on heat transfer in turbulent flow. For pulsating flows which may be considered to be quasi-steady, a condition which is attained in the limit of very small frequencies, the average Nusselt number was found to be less than the corresponding steady flow Nusselt number.

Krasuk and Smith (3) presented results of experiments on mass transfer in pulsating flow in a circular tube. They also presented an analogy between mass and momentum transfer which is shown to agree with their results.

A theoretical approach to the problem was first given by Lighthill (4). He studied the effect of small fluctuations in the free stream velocity on the momentum and thermal boundary layers along a solid body in unconfined flow. His method consisted of perturbing the solution to the steady flow problem. He considered only the linear term in the perturbation expansion, and as a result the change in time-averaged interphase flux was not obtained in his work.

The method presented in this paper employs a perturbation method similar to that used by Lighthill. In this study terms up to the second-order in the perturbation parameter were retained. Solutions of the differential equations for the individual terms in the perturbation expansion were then sought in the regions of high frequency and low frequency. The method was applied to the case of a steady laminar flow in a rigid tube upon which is superimposed a pressure gradient fluctuation which is a periodic function of time only. In a subsequent paper, the work will be extended to the problem of diffusion in a distensible tube, the pressure gradient disturbance being a wave traveling

in the direction of flow. The latter case would be of primary interest in the cardiovascular system.

PULSATING FLOW IN A RIGID TUBE

The solution for the simplest case of pulsating laminar flow in a rigid tube in which entrance effects are neglected has been known since the early work by Sexl (6). The equation of motion is given by

$$\frac{\partial u}{\partial t} = -\frac{1}{\rho} \frac{\partial p}{\partial x} + \frac{\nu}{r} \frac{\partial}{\partial r} r \frac{\partial u}{\partial r} \quad (1)$$

Let the average pressure gradient $(dp/dx)_0$ be disturbed by a simple sinusoidal form of fluctuation

$$-\frac{\partial p}{\partial x} = -\left(\frac{dp}{dx}\right)_0 (1 + \lambda \cos \beta t) \quad (2)$$

where $\lambda(dp/dx)_0$ is the amplitude of the pulsation and β its frequency. The solution of Equation (1) consists of a steady component u_0 and a transient component u_1 which is a periodic function of time. The component u_0 is given by the well-known Poiseuille flow relation

$$u_0 = 2U_0 \left(1 - \frac{r^2}{R^2}\right) \quad (3)$$

where U_0 is the time-averaged mean axial velocity. The fluctuating component is given by

$$u_1 = -\frac{8iU_0\lambda}{\omega^2} \left\{ 1 - \frac{J_0\left(\omega \frac{r}{R} i^{3/2}\right)}{J_0(\omega i^{3/2})} \right\} e^{i\beta t} \quad (4)$$

It is understood, of course, that only the real part of the above expression has physical significance. The symbol ω is the dimensionless frequency parameter, $\omega = (\beta R^2/\nu)^{1/2}$. J_0 denotes the Bessel function of order zero. Wormersley (8) discusses this solution and gives an extension to the case of a distensible conduit.

When the Schmidt number, ν/D , is very large (the Schmidt number for liquids is of the order 10^3 to 10^4), the hydrodynamic inlet region is much shorter than the diffusion inlet region. In most cases the ratio of the length of the diffusion inlet region to the length of the hydrodynamic inlet region is of such magnitude that for practical purposes the entire conduit may be treated as fully developed hydrodynamically but that the diffusion boundary layer thickness is small (a diffusion inlet region).

The following analysis will apply specifically to the diffusion inlet region beyond the flow inlet region. In this region, the rapid changes in the concentration of the dissolved substance take place across a very thin layer adjacent to the wall, the concentration boundary layer. Within this layer the velocity profile may be considered as a linear function of the distance from the wall with a slope equal to the actual slope at the wall. Making use of this approximation then, the velocity distribution near the wall becomes

$$u(y, t) \cong \frac{4U_0y}{R} + \lambda \frac{U_0y}{R} \chi(\omega) e^{i\beta t} \quad (5)$$

where y is the distance from the wall, $R = r$, and $\chi(\omega)$ is a function of the frequency parameter ω :

$$\chi(\omega) = -\frac{8i^{1/2}}{\omega} \frac{J_1(\omega^{3/2})}{J_0(\omega^{3/2})} \quad (6)$$

Hence the boundary layer analysis is somewhat similar to that of an unconfined flow although the problem under consideration is associated with flow in a rigid circular tube.

CONCENTRATION DISTRIBUTION AND DIFFUSION

The boundary layer equation for the dimensionless concentration variable ϕ is

$$\frac{\partial \phi}{\partial t} + u \frac{\partial \phi}{\partial x} = D \frac{\partial^2 \phi}{\partial y^2} \quad (7)$$

The variable ϕ is a dimensionless concentration which is zero at the conduit wall and is unity at the inlet

$$\begin{aligned} \phi &= 1 \text{ at } x = 0 && \text{for all } t \text{ and } y \\ \phi &= 0 \text{ at } y = 0 && \text{for all } t \text{ and } x > 0 \\ \phi &= 1 \text{ at } y = \infty && \text{for all } t \text{ and } x > 0 \end{aligned} \quad (8)$$

A perturbation solution to the differential Equation (7) is sought in the form

$$\phi(x, y, t) = \phi_0(x, y) + \lambda \phi_1(x, y, t) + \lambda^2 \phi_2(x, y, t) + O(\lambda^3) \quad (9)$$

The separate equations for the terms in the perturbation expansion are then derived in the usual way by substituting (9) into (7), collecting terms of the same power in λ , and equating the coefficient of each power of λ to zero.

The basic term $\phi_0(x, y)$ is the solution for steady laminar flow with mean velocity U_0 . It is given by

$$\phi_0 = \frac{(12)^{1/3}}{\Gamma(1/3)} \int_0^\infty \exp\left(-\frac{4}{9}\eta^3\right) d\eta \quad (10)$$

where η is the dimensionless variable $y(U_0/RDx)^{1/3}$.

The method of solution for the first and second-order terms will be discussed briefly below. The method is discussed more fully in the Appendix and complete details with tabular results are reported elsewhere (1).

In each case separate asymptotic solutions are sought for the regions of high frequency and low frequency. In addition, the differential equations were solved directly by numerical finite difference methods for several intermediate values of the frequency.

First-Order Solution ϕ_1

The differential equation for the first order term $\phi_1(x, y, t)$ is

$$\frac{\partial \phi_1}{\partial t} + \frac{4U_0y}{R} \frac{\partial \phi_1}{\partial x} + \frac{U_0y}{R} \chi(\omega) \frac{\partial \phi_0}{\partial x} = D \frac{\partial^2 \phi_1}{\partial y^2} \quad (11)$$

The solution is a periodic function of time of the form

$$\phi_1(x, y, t) = f_1(x, y) e^{i\beta t} \quad (12)$$

It should be mentioned that the first-order solution can not yield information on the time averaged interphase flux. ϕ_0 is the steady state solution based on the average velocity, and the time average of ϕ_1 and of the derivatives of ϕ_1 is zero. Hence, the first-order term makes no contribution to the time averaged Nusselt number.

The time dependence in Equation (11) is eliminated by substituting the above form of the solution into the differential equation. The result is an equation for $f_1(x, y)$

$$\frac{\partial^2 f_1}{\partial y^2} - \frac{4U_0y}{RD} \frac{\partial f_1}{\partial x} - \frac{i\omega^2 f_1}{R^2} = \frac{U_0y}{RD} \chi(\omega) \frac{\partial \phi_0}{\partial x} \quad (13)$$

where $\bar{\omega} = \omega(N_{Sc})^{1/2}$.

The low frequency asymptotic solution is developed by another perturbation technique with ω^2 as the perturbation parameter.

$$f_1(x, y) = f_{10}(x, y) + \omega^2 f_{11}(x, y) + \omega^4 f_{12}(x, y) + O(\omega^6) \quad (14)$$

The method of solution for the functions f_{10} , f_{11} , and f_{12} is described in Appendix A and complete results are given elsewhere (1). The solution in terms of the derivative at the wall is

$$\begin{aligned} \frac{\partial f_1}{\partial \eta} \Big|_{\eta=0} &= \frac{(12)^{1/3}}{3\Gamma(1/3)} \left[1 + i\omega^2 \left(-\frac{1}{8} - 0.2255 \xi^{2/3} N_{Sc} \right) \right. \\ &\quad \left. + \omega^4 \left(-\frac{1}{48} - \frac{0.2255}{8} \xi^{2/3} N_{Sc} \right) \right] \end{aligned} \quad (15)$$

The high frequency asymptotic solution is found using the theory of differential equations containing a large parameter. The procedure and principal results are discussed in Appendix A. The result in terms of the derivative at the boundary is

$$\begin{aligned} \frac{\partial f_1}{\partial \eta} \Big|_{\eta=0} &= \frac{(12)^{1/3}}{3\Gamma(1/3)} \\ &\quad \left(\frac{U_0}{RDx} \right) \chi(\omega) \int_0^\infty y^2 \exp\left(-\frac{\bar{\omega} i^{1/2} y}{R} - \frac{4}{9} y^3 \frac{U_0}{RDx}\right) dy \end{aligned} \quad (16)$$

The intermediate frequency solutions were found by straightforward numerical integration of Equation (13) using a method adapted from Crank-Nicholson. Several solutions of varying grid size were used in the usual way to determine that satisfactory accuracy was obtained.

The Second-Order Term ϕ_2

The differential equation for ϕ_2 is

$$\frac{1}{D} \frac{\partial \phi_2}{\partial t} + \frac{4U_0y}{RD} \frac{\partial \phi_2}{\partial x} + G(x, y, t) = \frac{\partial^2 \phi_2}{\partial y^2} \quad (17)$$

where the inhomogeneous term, $G(x, y, t)$, is given by

$$G(x, y, t) = \frac{U_0y}{RD} \operatorname{Re}[\chi(\omega)e^{i\beta t}] \operatorname{Re}\left(\frac{\partial f_1}{\partial x} e^{i\beta t}\right) \quad (18)$$

Study of this inhomogeneous term reveals that the second-order term consists of a time-independent term and a term which is a periodic function of time.

$$\phi(x, y, t) = M(x, y) + f_2(x, y) e^{2i\beta t} \quad (19)$$

Substitution of this form of the solution into the differential equation for ϕ_2 gives two separate equations for M and f_2 .

$$\frac{\partial^2 M}{\partial y^2} - \frac{4U_0 y}{RD} \frac{\partial M}{\partial x} = \frac{U_0 y}{2RD} \left\{ \operatorname{Re}[\chi(\omega)] \operatorname{Re} \left(\frac{\partial f_1}{\partial x} \right) + \operatorname{Im}[\chi(\omega)] \operatorname{Im} \left(\frac{\partial f_1}{\partial x} \right) \right\} \quad (20)$$

$$\frac{\partial^2 f_2}{\partial y^2} - \frac{4U_0 y}{RD} \frac{\partial f_2}{\partial x} - \frac{2i\omega^2 f_2}{R^2} = \frac{U_0 y}{2RD} \chi(\omega) \frac{\partial f_1}{\partial x} \quad (21)$$

The solution of Equation (20) for $M(x, y)$ is of considerable interest since $\partial M / \partial y|_{y=0}$ yields the time averaged flux due to the pulsation. For the high frequency asymptote, the Laplace transform of the equation is solved for the transform of M . Then the derivative of the transform is inverted by the method of convolution. Finally, the convolution integral may be approximated by

$$\frac{\partial M}{\partial \eta} \Big|_{\eta=0} = -\frac{8(12)^{1/3}}{3\Gamma(1/3)} \left[\frac{M_1(\omega)}{\omega M_0(\omega)} \right]^2 \frac{U_0}{RDx} \int_0^\infty y^2 \exp \left(-\frac{4}{9} y^3 \frac{U_0}{RDx} - \frac{\bar{\omega} y}{R\sqrt{2}} \right) \cos \left(\frac{\bar{\omega} y}{R\sqrt{2}} \right) dy \quad (22)$$

Appendix B gives more information on this solution.

For low frequencies, the function G becomes a particularly simple form such that the solution for M is a function of the variable η alone. The dimensionless derivative of M at the wall is given by

$$\frac{\partial M}{\partial \eta} \Big|_{\eta=0} = -\frac{(12)^{1/3}}{18\Gamma(1/3)} \left(1 - \frac{11\omega^4}{192} \right) \quad (23)$$

The transient term of $\phi_2(x, y, t)$ is derived in the same manner as $\phi_1(x, y, t)$ hence, only the final results of the mathematical operations will be presented here.

High frequency solution:

$$\frac{\partial f_2}{\partial \eta} \Big|_{\eta=0} = \frac{(12)\sqrt{2}}{12\Gamma(1/3)} \left[\frac{8M_1(\omega)}{\omega M_0(\omega)} \right]^2 \left\{ \left(\frac{U_0}{RDx} \right)^2 \frac{R^3}{\bar{\omega}^3} \exp \left\{ i \left[\theta_1(\omega) - \theta_0(\omega) + \frac{3\pi}{4} \right] \right\} \times \left\{ 4 \int_0^\infty \left(-\frac{4}{3} y^2 + \frac{4}{9} y^5 \frac{U_0}{RDx} \right) \exp \left(-\frac{\bar{\omega} i^{1/2} y}{R} - \frac{4}{9} y^3 \frac{U_0}{RDx} \right) dy - \int_0^\infty \left(\frac{\bar{\omega} i^{1/2} y \sqrt{2}}{R} + 4 \right) \left(-\frac{4}{3} y^2 + \frac{4}{9} y^5 \frac{U_0}{RDx} \right) \exp \left(-\frac{\bar{\omega} i^{1/2} y \sqrt{2}}{R} - \frac{4}{9} y^3 \frac{U_0}{RDx} \right) dy \right\} \right\} \quad (24)$$

Low frequency solution:

$$\frac{\partial f_2}{\partial \eta} \Big|_{\eta=0} = \frac{(12)^{1/3}}{18\Gamma(1/3)} \left[-1 + 0.8222\xi^{2/3} N_{Sc} i\omega^2 \left(1 - \frac{i\omega^2}{4} \right) \right] \quad (25)$$

RESULTS

The most interesting result in many applications is the Nusselt number or dimensionless mass flux. Some of the results in terms of this flux variable will be discussed in

this paper and complete results are available (1).

Range of Validity

A qualitative discussion of the validity of the boundary layer approach was given earlier. It can be shown (1) that the approximate range of applicability is given by

$$0.1 N_{Re} < \frac{x}{R} < 0.3 N_{Sc} N_{Re}$$

which of course, covers an x/R range of about four orders of magnitude in liquids. The results are also of value for heat transfer problems provided the Prandtl number (which replaces the Schmidt number in the usual way) is large as is the case in viscous liquids.

The perturbation method of solution must also be examined to determine the range of applicability. A second-order perturbation expansion, as given by Equation (9) is expected to be valid on condition that

$$\lambda^2 \phi_2(x, y, t) \ll \lambda \phi_1(x, y, t)$$

The perturbation method therefore imposes some restrictions on the magnitude of λ . The approximation unquestionably holds for values of λ approaching zero. And, if $\phi_2(x, y, t)$ is very small compared to $\phi_1(x, y, t)$ as in this case, then the parameter may be considerably increased without violating the perturbation limitations. An estimate of the allowable range of λ may be obtained from Figure 1, where the ratio $f_1/(|M| + |f_2|)$ at the point ($\eta = 2.0$, $\xi = 0.20 \times 10^{-2}$) is plotted as a function of ω . Smaller values of η would give curves above that of $\eta = 2.0$. The function $0.1 f_1/(|M| + |f_2|)$ is also shown on Figure 1, and values of η below this line may be considered as permissible values of λ .

An additional restriction on application of the results

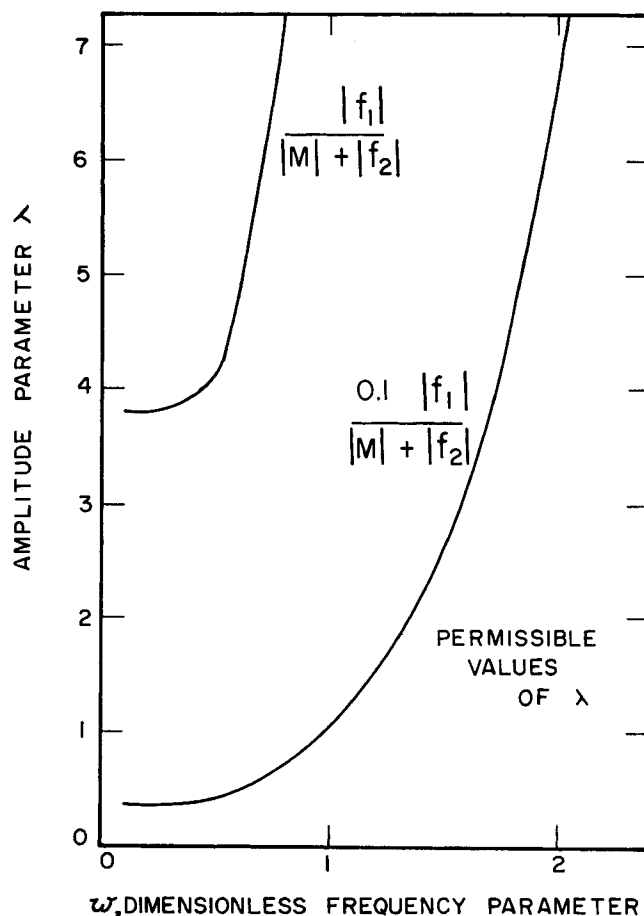


Fig. 1. Range of validity of the perturbation solution.

follows from the first of Equations (8). This equation is a boundary condition which implies no backflow or no convection of the concentration differences due to diffusion into the region of negative x . From Equation (4) it is easy to show that to avoid backflow it is necessary that

$$\lambda \leq \frac{\omega M_0(\omega)}{2M_1(\omega) \cos(\theta_1 - \theta_0 - \pi/4)} \quad (26)$$

which may be approximated with less than 15% error for $\omega > 4$ by $\lambda < \omega/\sqrt{2}$. Equation (26) is more restrictive than Figure 1 for values of ω greater than about 1.7. Unfortunately in previous work the few experiments which have been reported in detail have been under conditions which do not satisfy the inequality (26). These experiments show higher interphase fluxes than would be predicted by the model under consideration.

The Interphase Flux

Under the conditions of low concentration of diffusing species the interphase mass transfer is given by

$$J = -D(c_o - c_w) \frac{\partial \phi}{\partial y} \bigg|_{y=0}$$

or in terms of the Nusselt number

$$N_{Nu} = \frac{2RJ}{D(c_w - c_o)} = 2R \frac{\partial \phi}{\partial y} \bigg|_{y=0} \quad (27)$$

This expression may be placed in terms of the results reported here as

$$N_{Nu} = 2R \frac{\partial \phi_0}{\partial y} \bigg|_{y=0} + 2R\lambda \frac{\partial \phi_1}{\partial y} \bigg|_{y=0} + 2R\lambda^2 \frac{\partial \phi_2}{\partial y} \quad (28a)$$

$$N_{Nu} = N_{Nu}^{(0)} + \lambda N_{Nu}^{(1)} + \lambda^2 N_{Nu}^{(2)} \quad (28b)$$

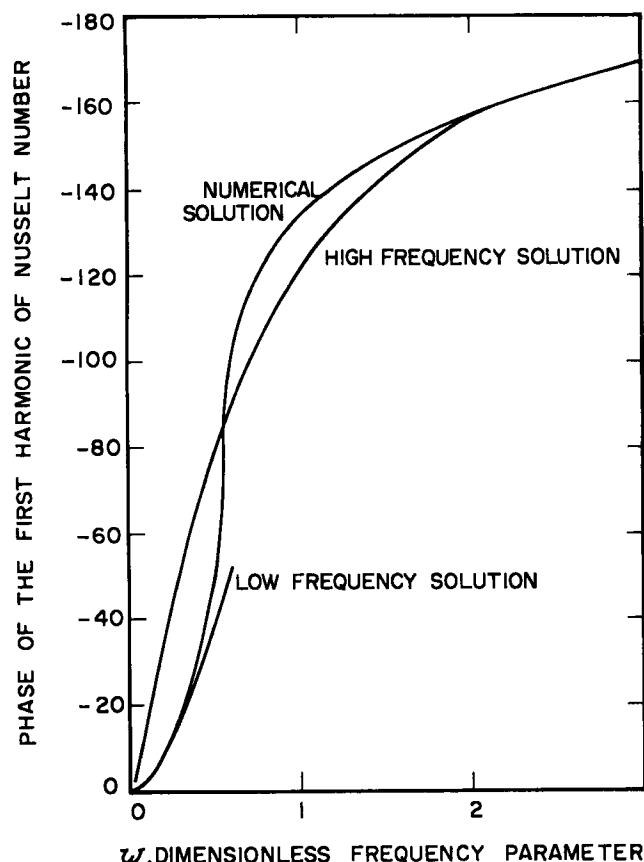


Fig. 2. Frequency dependence of the phase of the first harmonic of the Nusselt number [phase of $N_{Nu}^{(1)}$ for $\xi = 0.20 \times 10^{-2}$].

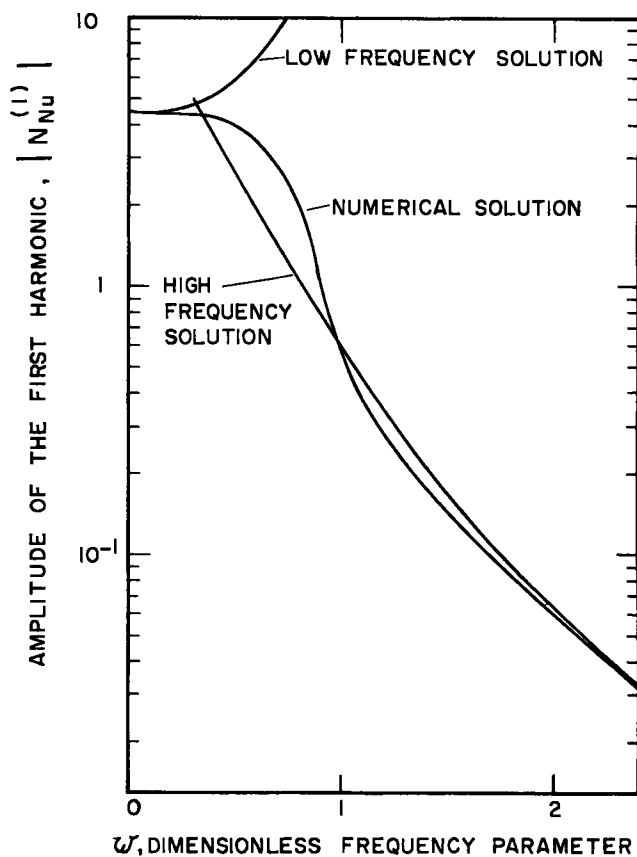


Fig. 3. Frequency dependence of the amplitude of the first harmonic of the Nusselt number [amplitude of $N_{Nu}^{(1)}$ for $\xi = 0.20 \times 10^{-2}$].

The N_{Nu} depends on the time variable, βt , the space variable ξ , the frequency parameter, ω , and the amplitude parameter, λ .

The first term in Equation (28) is designated as $N_{Nu}^{(0)}$ and corresponds to the Nusselt number for a steady flow with the same mean velocity. $N_{Nu}^{(0)}$ depends only on ξ .

$$N_{Nu}^{(0)} = \frac{2(12)^{1/3}}{\Gamma(1/3)} \xi^{-1/3} \quad (29)$$

The second term in Equation (28) is designated as $\lambda N_{Nu}^{(1)}$, the first order term or first harmonic.

$$N_{Nu}^{(1)} = 2\xi^{-1/3} \frac{\partial f_1}{\partial \eta} \bigg|_{\eta=0} e^{i\beta t} \quad (30)$$

$N_{Nu}^{(1)}$ is a periodic function with a zero time average. The phase lead (referred to a cosine wave of frequency β) and amplitude of the function are presented in Figures 2 and 3. The phase of the first harmonic of the flux lags behind that of $[-(1/\rho)(\partial p/\partial x)]$. This phase lag approaches π as the frequency of fluctuation becomes infinite. The amplitude decreases to zero at infinite frequency. These results are consistent with Lighthill in his study on a growing momentum boundary layer.

The third term in Equation (28) is designated as $\lambda^2 N_{Nu}^{(2)}$, the second order term. This term is divided in two functions as outlined previously,

$$N_{Nu}^{(2)} = N_{Nu}^{(2)}(t) + \overline{N_{Nu}^{(2)}} \quad (31)$$

$N_{Nu}^{(2)}(t)$ is a periodic function of time with a zero time average and is designated as the second harmonic

$$N_{Nu}^{(2)}(t) = 2\xi^{-1/3} \frac{\partial f_2}{\partial \eta} \bigg|_{\eta=0} e^{2i\beta t} \quad (32)$$

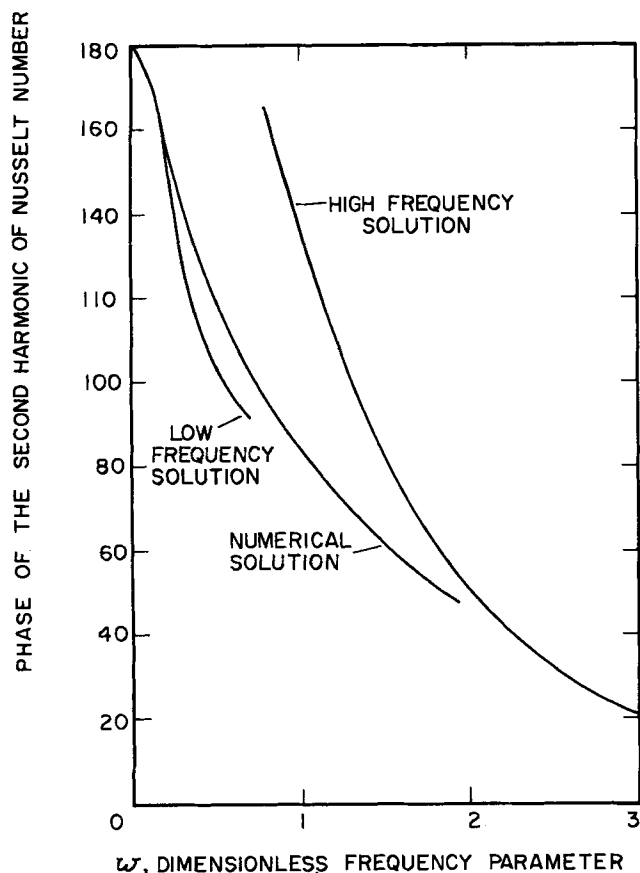


Fig. 4. Frequency dependence of the phase of the second harmonic of the Nusselt number [phase of $N_{Nu}^{(2)}(t)$ for $\xi = 0.20 \times 10^{-2}$].

The phase lead (referred to a cosine wave of the same frequency) and amplitude of this function are displayed in Figures 4 and 5. The phase of this function goes from π at zero frequency to zero at infinite frequency. The amplitude goes to zero at infinite frequency and decreases at a faster rate than the amplitude of the first harmonic.

The final and most important part, $N_{Nu}^{(2)}$ represents the increase in time-averaged Nusselt number due to the pulsations.

The time-averaged Nusselt number is given by

$$\bar{N}_{Nu} = N_{Nu}^{(0)} + \lambda^2 \overline{N_{Nu}^{(2)}} = N_{Nu}^{(0)} + 2\lambda^2 \xi^{-1/3} \left. \frac{\partial M}{\partial \eta} \right|_{\eta=0} \quad (33)$$

where $N_{Nu}^{(0)}$ is the Nusselt number in steady laminar flow with mean velocity U_0 . Curves of the increase in the Nusselt number for high and low frequency regions at a particular point along the conduit $\xi = 0.20 \times 10^{-2}$, are shown in Figure 6. The effect of axial position on the increase in \bar{N}_{Nu} is given in Figure 7.

The time-averaged Nusselt number in pulsating flow is affected by several factors, namely, the amplitude of the fluctuation, the frequency of the fluctuation and the position along the conduit. Each of these factors will be discussed in turn.

For very low frequencies, a rather surprising result was obtained. A sinusoidal pressure gradient causes the time-averaged Nusselt number to be less than that for steady flow at the same time-averaged rate. This unexpected result was verified by considering the behavior of the concentration boundary layer to be equivalent to a succession of steady states as the frequency approaches zero. The steady state equation for the concentration was solved using the instantaneous value of the velocity. The concentration was then averaged over one period. The Nusselt

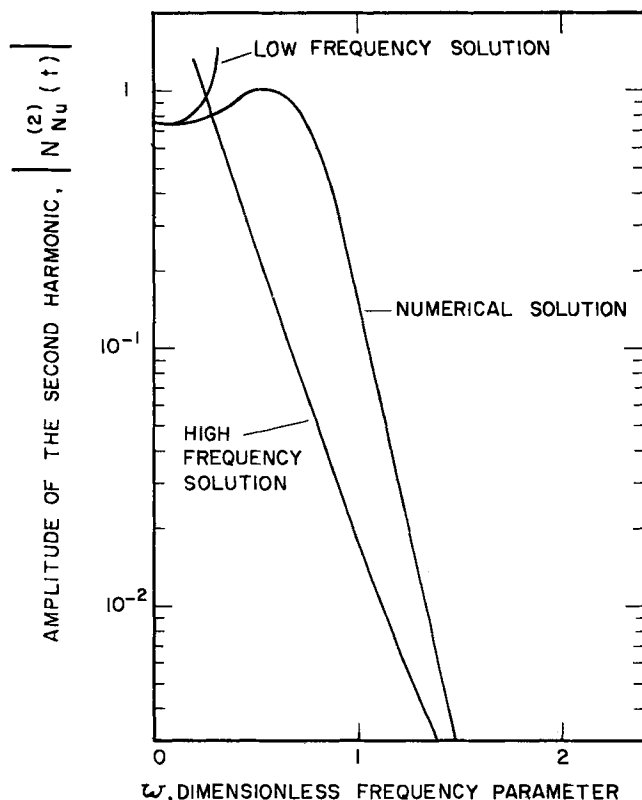


Fig. 5. Frequency dependence of the amplitude of the second harmonic of the Nusselt number [amplitude of $N_{Nu}^{(2)}(t)$ for $\xi = 0.20 \times 10^{-2}$].

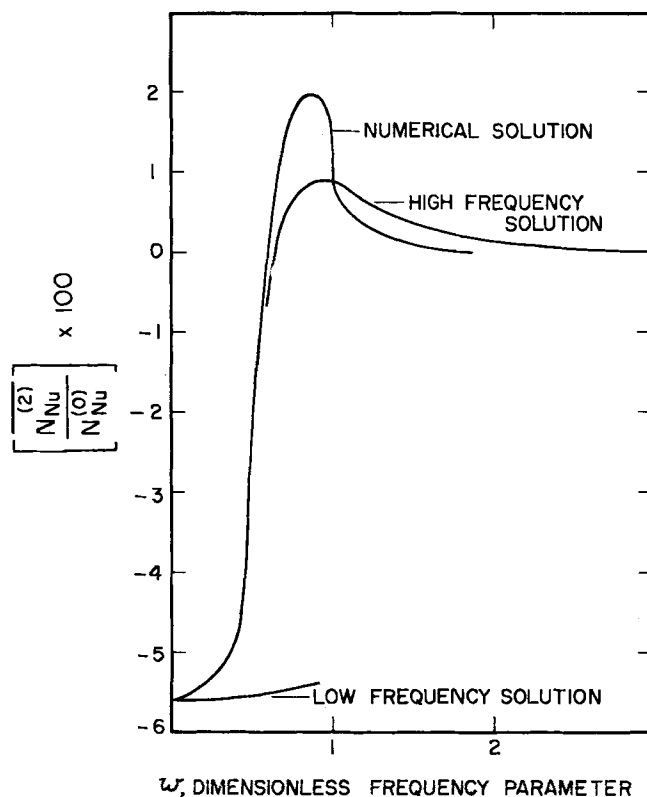


Fig. 6. Frequency dependence of the increase in the time averaged Nusselt number over the steady flow value for $\xi = 0.20 \times 10^{-2}$.

number derived in this manner for $\beta \rightarrow 0$ agreed with that obtained using the method presented in this paper.

For high frequencies, the change in \bar{N}_{Nu} due to pulsation is positive beyond a certain critical frequency and negative below it. The increase in \bar{N}_{Nu} goes through a maximum at some frequency above the critical frequency

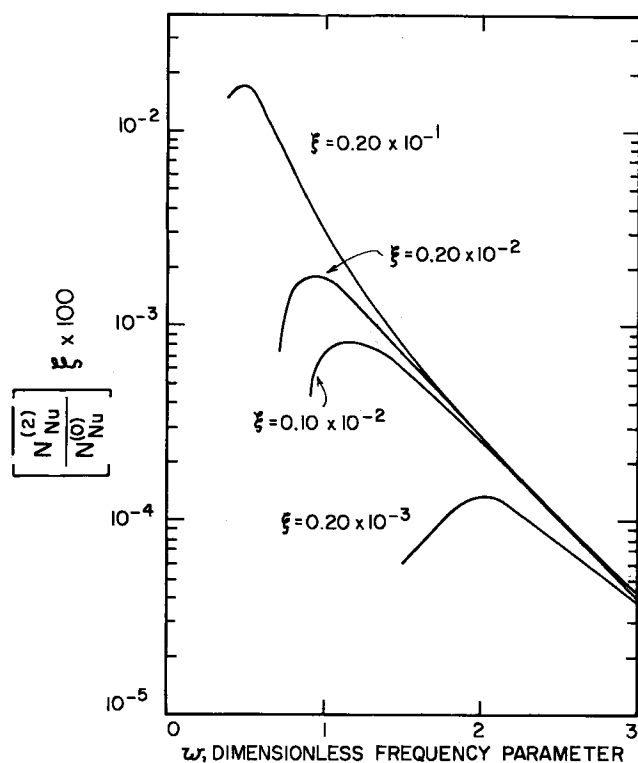


Fig. 7. Effect of axial position on the increase in the time averaged Nusselt number over the steady flow value.

and decreases to zero as the frequency becomes infinitely large.

The change in $\overline{N_{Nu}}$ is proportional to λ^2 within the range of validity of the perturbation solution. An increase in λ would bring about a greater increase or decrease in $\overline{N_{Nu}}$ depending on whether the frequency of fluctuation is above or below the critical frequency.

In the region of low frequencies, the change in $\overline{N_{Nu}}$ over the steady flow value, $(N_{Nu}^{(2)}/N_{Nu}^{(0)})$ is independent of ξ , the dimensionless x variable. But for very high frequencies $(N_{Nu}^{(2)}/N_{Nu}^{(0)})$ becomes inversely proportional to ξ .

The position of the critical frequency is likewise dependent on ξ . It tends to shift in the direction of decreasing frequency as ξ becomes larger.

It is often useful to consider space-averaged mass transfer rates rather than the local values discussed above. The asymptotic expression for high frequencies can be reduced to the simple form given below

$$\frac{F-1}{\lambda^2} = \frac{16\sqrt{2}}{3N_{Sc}^{3/2}\omega^5\xi_1^{1/3}\xi_2^{2/3}} \left[\frac{1-(\xi_1/\xi_2)^{1/3}}{1-(\xi_1/\xi_2)^{2/3}} \right]$$

where F denotes the ratio of the space (and time) averaged Nusselt number to the space-averaged Nusselt number for steady flow and $\xi_2 > \xi_1$.

ACKNOWLEDGMENT

This work was supported by NSF Grant GK 79 and by PHS Grant HE 09251.

NOTATION

c	= concentration
c_o	= uniform concentration at inlet
c_w	= constant concentration at wall
D	= diffusion coefficient
J	= interphase molar flux
$M_1(\omega)$	= modulus of the Bessel function $J_1(\omega t^{3/2})$
$M_0(\omega)$	= modulus of the Bessel function $J_0(\omega t^{3/2})$
N_{Nu}	= Nusselt number
N_{Re}	= Reynolds number

N_{Sc} = Schmidt number
 R = radius of the conduit
 U_0 = time-averaged mean axial velocity
 $Re(z)$ = the real part of the complex quantity z
 $Im(z)$ = the imaginary part of the complex quantity z

Greek Letters

β	= frequency in radians per unit time
η	= dimensionless variable, $y(U_0/RDx)^{1/3}$
θ_1	= phase of the Bessel function, $J_1(\omega t^{3/2})$
θ_0	= phase of the Bessel function, $J_0(\omega t^{3/2})$
λ	= ratio of amplitude of fluctuating component of the pressure gradient to the magnitude of the steady component
ν	= kinematic viscosity
ξ	= dimensionless x variable, Dx/U_0R^2
ϕ	= dimensionless concentration variable ($c - c_w$)/($c_o - c_w$)
χ	= function of ω , $[-(8i^{1/2}/\omega) J_1(\omega t^{3/2})/J_0(\omega t^{3/2})]$
ω	= dimensionless frequency parameter, $(\beta R^2/\nu)^{1/2}$
$\bar{\omega}$	= dimensionless frequency parameter, $(\beta R^2/D)^{1/2}$

LITERATURE CITED

- Alabastro, E. B. F., Ph.D. thesis, Rice Univ., Houston, Tex. (1967).
- Havemann, H. A., and N. N. Narayan Rao, *Nature*, **174**, 41 (1954).
- Krasuk, J. H., and J. M. Smith, *Chem. Eng. Sci.*, **18**, 591 (1963).
- Lighthill, M. J., *Proc. Roy. Soc. (London)*, **A224**, 1 (1954).
- Mueller, M. K., *Proc. Midwestern Conf. Fluid Mech.*, 5th, Ann Arbor, 146 (1957).
- Sext, T., *Z. Phys.*, **61**, 349 (1930).
- West, F. B., and A. T. Taylor, *Chem. Eng. Progr.*, **48**, 39 (1952).
- Womersley, J. R., *J. Physiology*, **127**, 553 (1955).

Manuscript received August 7, 1967; revision received February 29, 1968; paper accepted March 1, 1968.

APPENDIX A

Outline of Solutions for the First-Order Term, ϕ_1

Solutions for f_{10} , f_{11} , and f_{12} in the form of an expansion

$$f_{1n}(\eta, \xi) = \sum_{j=0}^{\infty} (\xi^{2/3})^j F_{nj}(\eta) \quad n = 0, 1, 2 \quad (A1)$$

are sought where ξ is the dimensionless x variable (Dx/U_0R^2). In practice, ξ is considerably less than unity and it will usually suffice to take only a few terms in the series. In this case, only the first two terms are found. Substitution in the usual way leads to second-order ordinary differential equations for F_{n0} and F_{n1} . The equations have solutions which are series expansions about $\eta = 0$ with infinite radii of convergence. However, for a large value of η , these series converge with discouraging slowness. For this reason asymptotic solutions for large η are derived. The asymptotic solution and the direct series expansion are then patched numerically at some intermediate value of η . This point was taken as the width of the unperturbed concentration boundary layer, $\eta_1 = \Gamma(1/3)/(12)^{1/3}$. The zero condition at the wall is imposed on the series expansion leaving one constant still undetermined. Similarly, the asymptotic expansion is made to satisfy the boundary condition at $\eta = \infty$. Since only one boundary condition is imposed the second constant in the asymptotic expansion is also unknown. To get the values of the constants, one from the series expansion and another from the asymptotic solution, the value of the function F_{nk} at η_1 , as given by the series solution is equated to that given by the series solution is equated to that given by the asymptotic solution. The derivatives of F_{nk} at η_1 are likewise equated giving two algebraic equations involving the two unknown constants.

The derivative of f_1 at the wall which applies to the low frequency region, is derived from the series solution of f_1 and is given by Equation (15).

To obtain the dominant term of the high frequency solution

